Mid-Infrared Silicon-on-Insulator Fourier-Transform Spectrometer Chip

Milos Nedeljkovic, Aitor V. Velasco, Ali Z. Khokhar, André Delâge, Pavel Cheben, and Goran Z. Mashanovich

Abstract— **Mid-infrared absorption spectroscopy is highly relevant for a wide range of sensing applications. In this letter, we demonstrate a Fourier-transform spectrometer chip based on the principle of spatial heterodyning implemented in the silicon-on-insulator waveguide platform, and operating near 3.75-μm wavelength. The spectrometer comprises a waveguide splitting tree feeding to an array of 42 Mach–Zehnder interferometers with linearly increasing optical path length differences. A spectral retrieval algorithm based on calibration matrices is applied to the stationary output pattern of the array, compensating for any phase and amplitude errors arising from fabrication imperfections. A spectral resolution below 3 nm is experimentally demonstrated.**

Index Terms— **Silicon photonics, spectroscopy, infrared.**

I. Introduction

THE FIELD of mid-infrared spectroscopy has witnessed a recent burst of research activity, predominantly in biological, chemical, and gas sensing sectors. Its applications include environmental sensing [1], breath analysis [2] and stand-off detection for security [3], to name a few. Existing mid-infrared spectrometers are bulky, expensive, and rely on lengthy scans, which ultimately limits their applicability.

Group-IV material waveguide platforms have an excellent potential for developing compact and cheap integrated mid-infrared spectroscopy systems [4]. Silicon-on-insulator (SOI) has already shown promising performance for wavelengths up to 4 μm, with strip waveguide losses of 1.3 dB/cm at 3.8 μm [5]. Germanium-on-silicon rib waveguides, with a loss as low as 0.6 dB/cm at 3.8 μm [6], are promising for low loss transmission over a very broad wavelength range (2-15 μm). Multimode interferometers [6]–[8], Mach-Zehnder interferometers (MZI) [7], [8], arrayed waveguide gratings (AWG) [9], [10] and planar concave grating (PCG) [9], [11] multiplexers have also been demonstrated in both platforms.

In this letter we demonstrate the first Fourier-transform (FT) SOI spectrometer chip operating in the mid-infrared. The device is based on the principle of spatial heterodyne spectroscopy (SHS) [12] in a planar waveguide configuration [13]. The spectrometer consists of an array of N Mach-Zehnder interferometers with linearly varying arm length differences, generating a stationary interferogram from which the input spectrum is recovered with FT-based techniques. The spectrometer chip builds upon a SHS configuration previously implemented in the near-infrared [14], incorporating a novel design of waveguides and optical elements to address specific challenges in the mid-IR, including efficient coupling and power splitting structures, and maintaining robust performance over a substantially broader Free Spectral Range (FSR). SHS enables a multi-aperture configuration with a separate input for each MZI, increasing optical throughput (étendue) N times compared to conventional waveguide integrated spectrometer devices such as AWGs and PCGs that require a single mode input waveguide. This greater étendue could be advantageous in spectroscopic applications relying on light from spatially extended or incoherent sources, or on an array of sources.

II. Design

In order to simplify testing, in this work we used a single input waveguide, followed by a splitting tree with several stages of cascaded −3dB splitters. This way the light is split into N waveguides, each feeding to a single 1×1 MZI. A grating coupler was used at each MZI output to monitor the interferometer transmission spectra. The maximum path length difference in the array (ΔL_{max}) and number of interferometers (N) determine the wavelength resolution ($\delta\lambda$) and FSR of the spectrometer:

$$\delta\lambda = \frac{\lambda_0^2}{\Delta L_{\max} n_g} \tag{1}$$

$$FSR = \delta\lambda \frac{N}{2} \tag{2}$$

where λ_0 is the device operational central wavelength and n_g is the waveguide group index.

We investigated two spectrometer layouts, both with $\Delta L_{max} = 1.383$ mm and $\delta\lambda = 2.8$ nm. The first

This work was supported by the Engineering and Physical Sciences Research Council through the MIGRATION project under Grant EP/L01162X/1. The work of A. V. Velasco was supported in part by the Spanish Ministry of Economy under Project TEC2012-37958-C02-02 and Project TEC2012-37958-C02-01, in part by the Community of Madrid under Project S2013/MIT-2790, and in part by The European Association of National Metrology Institutes through European Metrology Research Programme Project under Grant JRP IND14 FREQUENCY and PhotInd Project under Grant JRP-i22 IND22. The work of G. Z. Mashanovich was supported by the Royal Society through the University Research Fellowship.

M. Nedeljkovic, A. Z. Khokhar, and G. Z. Mashanovich are with the Optoelectronics Research Centre, University of Southampton, Southampton SO17 1BJ, U.K. (e-mail: m.nedeljkovic@soton.ac.uk; a.z.khokhar@soton.ac.uk; g.mashanovic@soton.ac.uk).

A. V. Velasco is with the Institute of Optics, Spanish National Research Council, Madrid 28006, Spain (e-mail: a.villafranca@csic.es).

A. Delâge and P. Cheben are with the National Research Council Canada, Ottawa, ON K1A 0R6, Canada (e-mail: andre.delage@nrc-cnrc.gc.ca; pavel.cheben@nrc-cnrc.gc.ca).

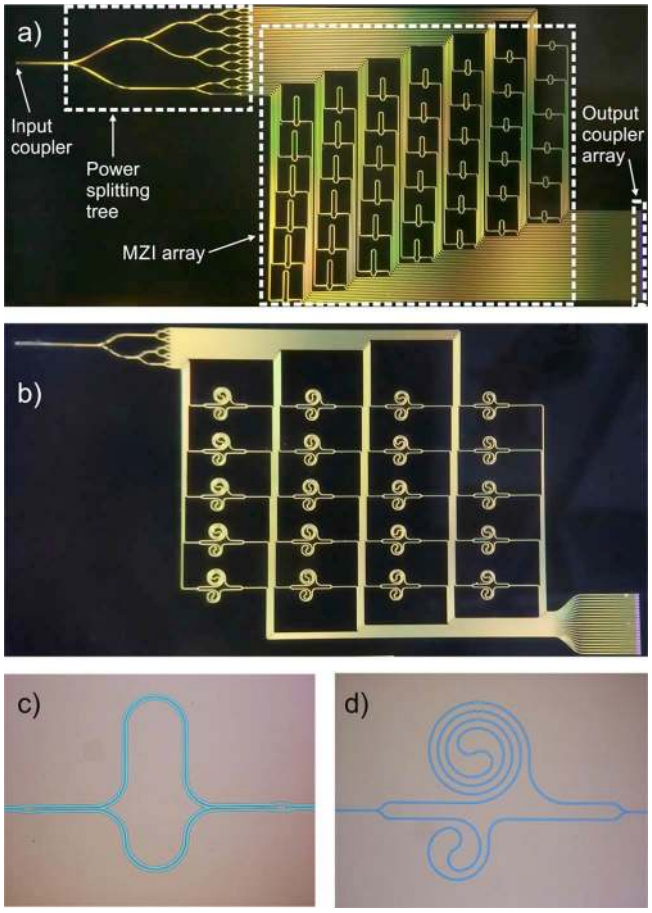

Fig. 1. Optical micrographs of a) FTIR1 spectrometer with conventional asymmetric MZIs, b) FTIR2 spectrometer with spiral-arm MZIs, c) conventional asymmetric MZI with MMI splitter and coupler, and d) spiral-arm asymmetric MZI with Y-junction splitter and coupler.

device (FTIR1), shown in Fig. 1a, comprises an array of 42 conventional 1×1 MZIs with straight arms (Fig. 1c) and has a footprint of 0.95 cm^2. 1×2 MMIs are used in both the splitting tree and the MZIs. The second device (FTIR2), which is shown in Fig. 1b, is an array of 20 1×1 MZIs with microphotonic spirals in both MZI arms (Fig. 1d) and has a footprint of 0.57 cm^2. Here Y-junction splitters and couplers were used in both the splitting tree and the MZIs. The longest spiral had an outer diameter of 340 μm. Both devices were optimized for the wavelength range 3715 - 3800 nm. The nominal FSRs of FTIR1 and FTIR2 were 58.8 nm and 28 nm, respectively.

Although both approaches are interchangeable in the devices under analysis, MMIs provide a greater fabrication tolerance and lesser insertion losses, while y-splitters present a broader bandwidth. FTIR2 has less interferometers than FTIR1 due to greater power-splitting losses and available optical power of the characterization setup. This limitation would nevertheless be circumvented in devices with multiple-aperture configurations [14]. MZIs in FTIR1 and FTIR2 present a similar footprint, but tightly coiled spiral arms would result in a more compact device for longer optical delays, at the cost of a small insertion loss penalty from waveguide bending.

SOI waveguides with nominal width (W) of 1350 nm, height (H) 400nm, etch depth (D) 220 nm, and

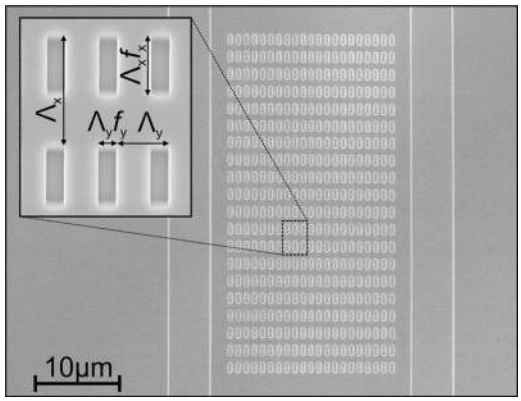

Fig. 2. SEM image of a grating coupler with sub-wavelength nanoholes. Detail view is shown in the inset, including the labels.

buried oxide (BOX) layer thickness (H_{BOX}) of 2 μm were used in the circuit. The 1×2 MMIs had tapered input and output ports, and the dimensions MMI width (W_{MMI}) of 8 μm, MMI length (L_{MMI}) 21.8 μm, output port separation (S) 4.18 μm, taper length (L_{tap}) 20 μm, and taper width (W_{tap}) 2.6 μm. Bend radii of 60 μm and 40 μm were used in the FTIR1 and FTIR2 designs, respectively. We have previously investigated the performance of the waveguides and coupling structure in this wavelength range [7].

We designed grating couplers for efficient coupling to and from the chip, using rectangular nanohole sub-wavelength (SWG) gratings, as first proposed by Halir et al. [15] and experimentally demonstrated in [16] and [17]. The SWG holes were designed for a 400 nm etch through the Si layer down to the BOX. In the direction parallel to waveguide light propagation the grating had a period (Λ_x) of 2.09 μm and fill factor (f_x) of 0.35, and in the perpendicular direction it had a period (Λ_y) 1 μm and a fill factor (f_y) 0.5. The coupler was designed using 2D Finite-Difference Time-Domain (FDTD) simulations in RSoft software. A SEM image of a fabricated grating coupler is shown in fig. 2, with labelled dimensions shown in the inset.

III. Experiment and Results

The devices were fabricated in two patterning and etch steps. First, a deep etch (400 nm) was used to form the grating coupler holes, and it was followed by a shallow (220 nm) etch for the interconnecting waveguides. For both steps, e-beam lithography using ZEP e-beam resist was used for pattern definition and the pattern was transferred to the silicon by inductively coupled plasma (ICP) etching.

A mid-IR setup comprising a tunable quantum cascade laser (transmission range 3715 – 3890 nm), an InSb detector, and fluoride fibers for coupling light between the laser, chip and detector, was used for all optical characterization measurements. The setup has been described in detail in [7] and [18]. To obtain the spatial interferogram, the transmission spectrum of each MZI output was measured independently. A Peltier stage was used for temperature stabilization to ±0.2 °K throughout the measurements.

The waveguide propagation loss was determined as 8.8 ± 0.5 dB/cm. This loss is larger than previously reported losses for the same waveguide dimensions [7], which is due to

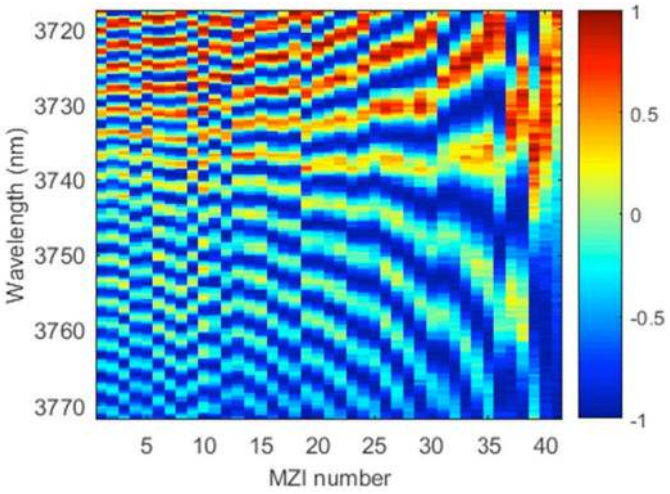

Fig. 3. Normalized amplitude of the experimental transmittance spectra for each of the 42 MZIs in the interferometer array on chip FTIR1; the wavelength range is 3717 nm – 3772 nm. Similar deviations of the ideal response are found for FTIR2.

a fabrication related issue in this specific run. MZI insertion losses were characterized by comparison with normalization structures with the same power-splitting trees. The straight-arm MZIs had insertion losses of 1.5 - 3.5 dB, whereas y-junctions proved to be too sensitive to fabrication variations to provide accurate references. We also characterized the wavelength sensitivity of the MZIs to thermal variations by measuring transmission spectra of a few MZIs at different temperature settings, which was controlled using the Peltier stage. The temperature induced shift in MZI fringes was found to be 180 pm/°K. Spectral responses of the grating couplers did not vary substantially between devices.

The measured transmittance spectra for all the Mach-Zehnder interferometers in the array (FTIR1) are shown in Fig. 3. A 2 dB extinction ratio variation due to MZI losses is observed along the array. Phase and amplitude deviations from the theoretical sinusoidal function of each MZI are caused by fabrication imperfections, propagation losses, uneven power-splitting and grating coupler spectral dependence. Similar deviations from the ideal response are found for FTIR2. All these interferogram distortions are numerically compensated in the spectral retrieval algorithm, by incorporating the calibrated transmittance spectra into a transformation matrix T. The input spectrum B of any arbitrary input signal is then retrieved by multiplying the interferogram I by the pseudoinverse of the transfer matrix T [14].

Figure 4 presents the experimentally retrieved spectra of a monochromatic input at several wavelengths along the FSR of both devices. Each line is retrieved with a resolution of 2.7 nm for FTIR1 and 2.9 nm for FTIR 2, measured at the full width at half-maximum (FWHM), presenting a good agreement with the theoretically predicted values. FSR of each device is measured to be 57 nm and 29 nm, in accordance with Eq. 2. Noise levels in the retrieved spectra are mainly caused by limitations of the experimental setup and the retrieval algorithm.

IV. Summary

In summary, we have demonstrated the first Fourier transform spatial heterodyne spectrometer chip in the mid-

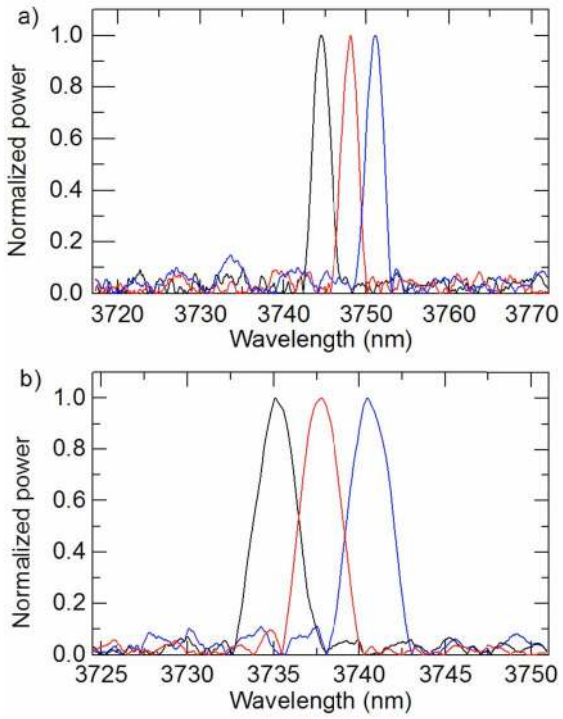

Fig. 4. Spectra of a narrowband laser tuned to three different wavelengths, experimentally retrieved with a) the FTIR1 chip, b) the FTIR2 chip. Resolutions of 2.7 nm and 2.9 nm are demonstrated, respectively, with FSRs of 57 nm and 29nm.

infrared. The spectral range of these spectrometers can readily be adapted to work at any wavelength range where SOI waveguides have low loss (i.e. $\lambda < \sim 4\ \mu$m) by re-optimizing waveguide design, enabling diverse applications in environmental sensing, breath analysis or stand-off detection for security. The design is inherently flexible, given that the resolution and FSR of the spectrometer can be increased by changing the path length differences and number of the MZIs, while its sensitivity is only limited by the resulting fringe visibility and the thermal stability of the device. Two alternative implementations for power-splitting and optical delays have been demonstrated, adding to the versatility of the spectrometer for diverse applications. MMIs provide reduced insertion losses in devices with a high number of interferometers, whereas y-junctions can operate over broader wavelength ranges. MZIs with spiral arms provide a more compact footprint for large resolutions. Furthermore, this approach should work equally well in other MIR waveguide platforms. Device operation could be improved by simultaneous monitoring of all of the spectrometer outputs with a MIR camera or, in an ideal future device, on-chip integrated detectors.

Acknowledgment

The data for this project can be found at http://dx.doi.org/10.5258/SOTON/383407.

References

[1] A. P. M. Michel *et al.*, "Quantum cascade laser open-path system for remote sensing of trace gases in Beijing, China," *Opt. Eng.*, vol. 49, no. 11, pp. 111125-1–111125-8, 2010.

[2] K. Wörle *et al.*, "Breath analysis with broadly tunable quantum cascade lasers," *Anal. Chem.*, vol. 85, no. 5, pp. 2697–2702, 2013.

[3] R. Furstenberg *et al.*, "Stand-off detection of trace explosives via resonant infrared photothermal imaging," *Appl. Phys. Lett.*, vol. 93, no. 22, p. 224103, 2008.
[4] R. Soref, "Mid-infrared photonics in silicon and germanium," *Nature Photon.*, vol. 4, pp. 495–497, Aug. 2010.
[5] G. Z. Mashanovich *et al.*, "Silicon photonic waveguides and devices for near- and mid-IR applications," *IEEE J. Sel. Topics Quantum Electron.*, vol. 21, no. 4, Jul./Aug. 2015, Art. ID 8200112.
[6] M. Nedeljkovic *et al.*, "Surface-grating-coupled low-loss Ge-on-Si rib waveguides and multimode interferometers," *IEEE Photon. Technol. Lett.*, vol. 27, no. 10, pp. 1040–1043, May 15, 2015.
[7] M. Nedeljkovic *et al.*, "Silicon photonic devices and platforms for the mid-infrared," *Opt. Mater. Exp.*, vol. 3, no. 9, pp. 1205–1214, 2013.
[8] A. Malik, M. Muneeb, Y. Shimura, J. Van Campenhout, R. Loo, and G. Roelkens, "Germanium-on-silicon mid-infrared waveguides and Mach-Zehnder interferometers," in *Proc. IEEE Photon. Conf. (IPC)*, Sep. 2013, pp. 104–105.
[9] M. Muneeb *et al.*, "Demonstration of silicon-on-insulator mid-infrared spectrometers operating at 3.8 μm," *Opt. Exp.*, vol. 21, no. 10, pp. 11659–11669, 2013.
[10] A. Malik *et al.*, "Germanium-on-silicon mid-infrared arrayed waveguide grating multiplexers," *IEEE Photon. Technol. Lett.*, vol. 25, no. 18, pp. 1805–1808, Sep. 15, 2013.
[11] A. Malik, M. Muneeb, Y. Shimura, J. Van Campenhout, R. Loo, and G. Roelkens, "Germanium-on-silicon planar concave grating wavelength (de)multiplexers in the mid-infrared," *Appl. Phys. Lett.*, vol. 103, no. 16, p. 161119, 2013.
[12] J. M. Harlander *et al.*, "Robust monolithic ultraviolet interferometer for the SHIMMER instrument on STPSat-1," *Appl. Opt.*, vol. 42, no. 15, pp. 2829–2834, 2003.
[13] M. Florjańczyk, P. Cheben, S. Janz, A. Scott, B. Solheim, and D.-X. Xu, "Multiaperture planar waveguide spectrometer formed by arrayed Mach-Zehnder interferometers," *Opt. Exp.*, vol. 15, no. 26, pp. 18176–18189, 2007.
[14] A. V. Velasco *et al.*, "High-resolution Fourier-transform spectrometer chip with microphotonic silicon spiral waveguides," *Opt. Lett.*, vol. 38, no. 5, pp. 706–708, 2013.
[15] R. Halir, P. Cheben, S. Janz, D.-X. Xu, Í. Molina-Fernández, and J. G. Wangüemert-Pérez, "Waveguide grating coupler with subwavelength microstructures," *Opt. Lett.*, vol. 34, no. 9, pp. 1408–1410, 2009.
[16] R. Halir *et al.*, "Continuously apodized fiber-to-chip surface grating coupler with refractive index engineered subwavelength structure," *Opt. Lett.*, vol. 35, no. 19, pp. 3243–3245, 2010.
[17] X. Chen and H. K. Tsang, "Nanoholes grating couplers for coupling between silicon-on-insulator waveguides and optical fibers," *IEEE Photon. J.*, vol. 1, no. 3, pp. 184–190, Sep. 2009.
[18] G. Z. Mashanovich *et al.*, "Low loss silicon waveguides for the mid-infrared," *Opt. Exp.*, vol. 19, no. 8, pp. 7112–7119, 2011.